

AperTO - Archivio Istituzionale Open Access dell'Università di Torino

The ZVI-Fenton process affects the total load of human pathogenic bacteria in wastewater samples

This is the author's manuscript

Original Citation:

Availability:

This version is available <http://hdl.handle.net/2318/1847282> since 2022-12-15T17:44:41Z

Published version:

DOI:10.1016/j.jwpe.2022.102668

Terms of use:

Open Access

Anyone can freely access the full text of works made available as "Open Access". Works made available under a Creative Commons license can be used according to the terms and conditions of said license. Use of all other works requires consent of the right holder (author or publisher) if not exempted from copyright protection by the applicable law.

(Article begins on next page)

1 **The ZVI-Fenton process affects the total load of human pathogenic bacteria in**
2 **wastewater samples**

3

4 **Raffaella Sabatino^a, Francesco Furia^{b,c}, Ester M. Eckert^a, Marco Minella^c, Gianluca**
5 **Corno^a, Andrea Di Cesare^{a*}, Davide Vione^{c*}**

6 *^a Water Research Institute (IRSA) - MEG Molecular Ecology Group, CNR - National Research*
7 *Council of Italy, Largo Tonolli 50, 28922, Verbania, Italy*

8 *^b Dipartimento attività produttive e impatto sul territorio – UOC Valutazione e Pareri*
9 *Ambientali - Arpa Sicilia, Viale Cristoforo Colombo snc, 90149, Palermo, Italy*

10 *^c Department of Chemistry, Università di Torino, Via Pietro Giuria, 5, 10125 Torino, Italy*

11

12 * Corresponding authors:

13 CNR – Water Research Institute, Largo Tonolli 50, 28922, Verbania, Italy. E-mail address,
14 *andrea.dicesare@cnr.it* (Andrea Di Cesare).

15 Department of Chemistry, Università di Torino, Via Pietro Giuria, 5, 10125, Torino, Italy. E-
16 mail address, *davide.vione@unito.it* (Davide Vione).

17

18 **Abstract**

19 We investigated the effectiveness of a heterogeneous Fenton-like reaction (ZVI-Fenton, i.e., ZVI
20 + H₂O₂, where ZVI = zero-valent iron) towards the removal of potentially pathogenic bacteria in
21 wastewater (WW). The effectiveness of the process was investigated towards live bacteria
22 (measured by flow cytometry) as well as potentially pathogenic bacteria (identified by 16S
23 rRNA amplicon sequencing), antibiotic resistance genes and class 1 integrons (assessed by
24 qPCR). The ZVI-Fenton process resulted about as effective as H₂O₂ alone to decrease live
25 bacteria ($p>0.05$), if compared with the blank controls (neither ZVI nor H₂O₂, $p=0.00005$),
26 although it did not reduce the relative abundance of the tested antibiotic resistance genes or class
27 1 integrons ($p>0.05$). However, ZVI-Fenton was quite effective in lowering the total content of
28 the potentially pathogenic bacteria in WW when compared to the controls with ($p=0.0186$) and
29 without H₂O₂ ($p=0.0252$). These findings suggest that ZVI-Fenton has potential as an effective
30 WW treatment technique that should be further investigated for future application in WWTPs.

31

32 **Keywords:** Zero Valent Iron; Fenton-like process; wastewater; pathogens; antibiotic resistance
33 genes; Advanced Oxidation Processes.

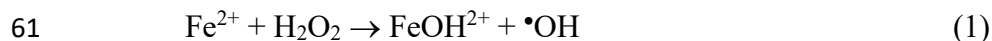
34

35 **1. Introduction**

36 In wastewater treatment plants (WWTPs), disinfection is the last step devoted to minimize the
37 pathogenic bacterial load (Di Cesare et al., 2020a). However, pathogenic bacteria can escape
38 disinfection processes and can thus be found in treated wastewaters (WWs), from which they
39 enter the aquatic environment (Shi et al., 2021). This is a serious concern for human health
40 because treated WW can become a source for waterborne diseases, depending on its further use
41 (Li et al., 2015). Furthermore, WWTPs are considered as hotspots of antibiotic resistance
42 (Berendonk et al., 2015) and represent a direct source of antibiotic resistant bacteria and
43 antibiotic resistance genes (ARGs) to the aquatic environment (Czekalski et al., 2014; Rizzo et
44 al., 2013). Once in the aquatic environment, pathogenic and/or antibiotic resistant bacteria can
45 infect humans through different ways that include skin contact, ingestion, as well as fish and
46 shellfish contamination (Arnone and Perdek Walling, 2006; Leonard et al., 2018). Therefore,
47 alternative and innovative disinfection processes should be investigated to improve the removal
48 of the total potential human pathogenic bacteria from the WW bacterial communities, to prevent
49 or reduce their release into the aquatic environment.

50 A possible future challenge for disinfection techniques is their coupling with depollution
51 processes, that is, the elimination of chemical contaminants. In particular, several Advanced
52 Oxidation Processes (AOPs) have been developed that rely on the production of strongly
53 oxidizing transient species such as the hydroxyl ($\bullet\text{OH}$) and sulfate ($\text{SO}_4^{\bullet-}$) radicals (Comninellis
54 et al., 2008; Mirzaei et al., 2017). AOPs are involved in the degradation of pollutants including
55 the contaminants of emerging concern (CECs), such as pharmaceuticals and personal care
56 products (Huber et al., 2003; Wang and Zhuan, 2020). CECs are hydrophilic and often
57 biorecalcitrant, and are usually not or incompletely removed by the traditional water treatment

58 methods (Richardson and Ternes, 2018). A common AOP is the Fenton reaction (1), which
59 involves water-soluble ferrous salts and hydrogen peroxide to produce $\bullet\text{OH}$ (as well as additional
60 oxidants such as ferryl, FeO^{2+}) (Pignatello et al., 2006, 1999):



62 Although it is cheap and easy to implement, the Fenton reaction has some important drawbacks:
63 first of all, it is most efficient at pH 3 (Pignatello et al., 2006) that is hardly attainable in water
64 treatment, due to both reagent costs and the salinity of treated water after the post-treatment
65 neutralization step. Moreover, neutralization yields an iron-rich precipitate sludge that cannot be
66 recycled in the process and has to be disposed of in some way (Huang et al., 2013). The addition
67 of iron ligands can keep Fe dissolved and avoid formation of precipitates while often improving
68 Fenton degradation, but it will cause issues with iron limits for wastewater discharge and will
69 shift reactivity from $\bullet\text{OH}$ to less reactive oxidant species such as ferryl, thereby hampering
70 degradation of some recalcitrant contaminants (Farinelli et al., 2020).

71 Several attempts have been made to improve the Fenton reaction, and one of the most promising
72 is heterogeneous Fenton. It consists in the replacement of soluble Fe^{2+} species with solid Fe-
73 based materials (Tang and Wang, 2020; Vorontsov, 2019), of which zero-valent iron (Fe^0 or
74 ZVI) is one of the cheapest and most robust in terms of application (GilPavas et al., 2019; Joo et
75 al., 2005; Rezaei and Vione, 2018). ZVI-Fenton also allows for water treatment to be carried out
76 at higher pH compared to traditional Fenton (Minella et al., 2016). In particular, ZVI-Fenton has
77 been shown to achieve effective degradation of pharmaceuticals (including hospital antibiotics)
78 in real wastewater at pH 5 or even 6 depending on the contaminant, with competitive treatment
79 costs (in the order of 0.04-0.1 \$ m^{-3} for the chemical reagents) (Furia et al., 2021; Minella et al.,

80 2019). Note that ZVI is a well-known reducing agent (Xu et al., 2019), but in the presence of
81 dissolved oxygen it can trigger the Fenton reaction (Fu et al., 2014). However, the effectiveness
82 of ZVI alone toward contaminant degradation (either reductive or oxidative) is only a very small
83 fraction of what is observed in the presence of ZVI + H₂O₂ (Furia et al., 2021).

84 The production of •OH makes the Fenton reaction potentially suitable for disinfection, because
85 •OH is also able to inactivate bacteria and viruses by damaging/destroying cell membranes or
86 viral capsids (Giannakis et al., 2016; McGuigan et al., 2012; Ruales-Lonfat et al., 2014). For
87 instance, Fenton-like techniques have been the object of considerable research in the framework
88 of the improvement of Solar Water Disinfection - SODIS (Carratalà et al., 2016; García-Gil et
89 al., 2021; Giannakis et al., 2018), which is a low-cost and solar-based disinfection of drinking
90 water that is often the only feasible water treatment option in developing countries.

91 For the above issues, it is very interesting to investigate if the Fenton process (carried out in
92 heterogeneous conditions through ZVI) can achieve both depollution from contaminants and
93 disinfection of pathogens in a two-birds-with-one-stone approach. Therefore, this contribution
94 considers ZVI-Fenton as an innovative and cheap AOP, which is able to effectively degrade
95 pharmaceuticals (including hospital antibiotics) at very competitive cost compared to traditional
96 Fenton or ozonation, to see if the same conditions that already gave promising results with
97 pollutant degradation in real wastewater (Furia et al., 2021) are also effective towards
98 disinfection.

99

100 **2. Materials and Methods**

101

102 *2.1 Wastewater*

103 The real WW sample used in this work was obtained from the secondary clarifier tank outflow of
104 an urban WWTP from Verbania (Piedmont, NW Italy, population equivalents of 51k inhabitants,
105 described in Di Cesare et al., 2016). The main chemical features of the studied WW sample are
106 reported in **Supplementary Table S1** of the Supplementary Material (hereinafter, SM). The
107 WW chemical characterization procedures are described in SM, **Paragraph S1**.

108

109 *2.2 Choice of operational conditions*

110 Although the Fenton reaction is most effective at pH 3 (Pignatello et al., 2006) and ZVI-Fenton
111 makes no exception (Furia et al., 2021), and although such pH conditions would effectively kill
112 practically all bacteria in wastewater, operation at pH 3 is not practical in an application
113 scenario. Indeed, apart from the cost of the acid that would be a major expense voice at pH 3
114 (Minella et al., 2018), one has to neutralize acidic pH before wastewater discharge. That
115 operation would (i) require a relatively high amount of a base with the associated costs, and (ii)
116 produce a saline stream that might pose problems for discharge or reuse. Operation at pH 4
117 would pose similar problems, although to a lesser extent, while ZVI-Fenton suffers from a
118 dramatic loss of effectiveness in wastewater between pH 6 and 7 (Minella et al., 2019). For these
119 reasons we chose to operate at pH 5 and 6, where previous work has shown that suitable
120 conditions can be found to achieve effective ZVI-Fenton degradation of antibiotics in

121 wastewater. Moreover, pH 5-6 allows for lower use of H_3PO_4 (*vide infra*) compared to pH 4,
122 thereby decreasing costs and facilitating phosphate elimination in a following step.

123

124 2.3 Microbiological experiments

125 The experimental design consisted of two parts, referred to as “experiment 1” and “experiment
126 2”, respectively (**Figure 1**). In the “experiment 1” we investigated the effect of the ZVI-Fenton
127 process at different pH values on bacterial abundance and vitality of a partially treated WW
128 microbial community. The aim was to select the best performing condition in terms of abatement
129 of cell number and reduction of cell vitality. In this case, the collected WW sample (pH 7.5) was
130 immediately transported to the laboratory. The sample was split in three equal aliquots and the
131 pH adjusted as follows (time = T0): (i) pH 5 with H_2SO_4 ; (ii) pH 5 with H_3PO_4 ; (iii) pH 6 with
132 H_3PO_4 . H_2SO_4 and H_3PO_4 are the only two inorganic acids that proved effective in the Fenton
133 process, considering that HCl is to be avoided because Cl^- scavenges $\bullet\text{OH}$ in acidic solution and
134 may thus inhibit Fenton degradation (Coha et al., 2021), while HNO_3 and HClO_4 are ruled out
135 because of high toxicity of the conjugated anions.

136 From each sub-sample, three series of flasks (each one in triplicate) were prepared, each
137 containing 50 mL of acidified WW. One set of flasks was untreated (control), the second one
138 was amended with H_2O_2 , and the third one with ZVI + H_2O_2 . The values of H_2O_2 concentration,
139 ZVI loading and their mode of addition, which may imply multiple additions during the course
140 of the reaction, are described in the **Supplementary Table S2**. These conditions were chosen
141 because of their effectiveness in degrading hospital antibiotics in WW (Furia et al., 2021; data of
142 hospital antibiotic degradation in the same conditions with the same wastewater are also shown

143 in **Table S2**). The flasks were incubated at room temperature for 90 min in the dark. The pH
144 value was monitored during treatment and, in case, corrected (**Supplementary Table S2**). At the
145 end of the treatment, 1 mL of a catalase solution (0.1 g L^{-1}) was added to each flask, to degrade
146 any potentially residual peroxide (the complete degradation of H_2O_2 was confirmed
147 spectrophotometrically). Then, samples were neutralized with NaOH (0.1 mol L^{-1}) up to pH 6 if
148 needed (time = T90S). Indeed, pH 6 is fully consistent with wastewater disposal into surface
149 waters (Salgot et al., 2006). An aliquot (1 mL) from each sub-sample was fixed with formalin
150 (final formaldehyde concentration 1.5%) and analyzed by flow cytometry.

151 The “experiment 2” had the aim of understanding how the selected ZVI-Fenton process affects
152 the load of potential human pathogenic bacteria and the antibiotic resistome (total content of
153 antibiotic resistance genes, ARGs) of the WW bacterial community. To do this “experiment 1”
154 was replicated in the conditions that proved most promising/effective in the first experimental
155 series, namely acidification at pH 5 with H_3PO_4 , except that the acidified WW volume was
156 increased to 350 mL and all the other reagents were added accordingly (**Supplementary Table**
157 **S2**). At the end of the procedure, preliminary sample characterization was carried out by flow
158 cytometry and, most notably, treated WWs and controls were processed for DNA extraction. An
159 aliquot of DNA was twofold diluted and used for quantitative real-time polymerase chain
160 reaction (qPCR) analysis. The other aliquot was processed for 16S rRNA gene amplicon
161 sequencing, and shipped under controlled conditions to an external company for sequencing
162 (IGA technologies, Padova, Italy). All the statistical analyses were conducted in the R
163 environment version 3.6.0 (R Core Team, 2019).

164

165 2.4 Flow cytometry

166 The total bacterial number and the proportion of damaged cells in formalin fixed sub-samples
167 were obtained using previously described protocols for cytogram design (Corno et al., 2013) and
168 intact/damaged cells identification (after staining with SYBR green and propidium iodide 1:1)
169 (Amalfitano et al., 2015). For comparison, the initial WW sample was analyzed by flow
170 cytometry, too. An ANOVA (Analysis of Variance, Tukey post-hoc tested) was performed, after
171 a log-transformation of the data, to test for significant differences ($p < 0.05$) between sample
172 series.

173

174 2.5 DNA extraction

175 A volume of 100 mL of Fenton-treated WWs and controls derived from “experiment 2” was
176 filtered onto 0.22 μm polycarbonate filters (Millipore). The filters were then processed for DNA
177 extraction using the DNeasy UltraClean Microbial Kit (Qiagen), according to the manufacturer’s
178 instructions. DNA was divided into two aliquots, and kept at -20°C before being treated as
179 described below.

180

181 2.6 Antibiotic resistance genes (ARGs) and *intI1* gene quantification

182 As a general proxy for anthropogenic pollution in aquatic environments, we quantified the
183 integrase gene of the class 1 integrons (*intI1*) (Gillings et al., 2015). ARGs that are widespread in
184 wastewater and aquatic ecosystems were selected for analysis, namely: *sul2*, *tetA* and *qnrS*
185 (coding for the resistance against sulfonamides, tetracyclines and quinolones, respectively) (Di

186 Cesare et al., 2015, 2016a; Galafassi et al., 2021; Sabatino et al., 2020). qPCR was used to
187 quantify the gene abundances, with the methodological details as described elsewhere (Di Cesare
188 et al., 2015), on a RT-thermocycler CFX Connect (Bio-Rad). The primer pair sequences and
189 annealing temperatures are detailed in Supplementary Table S3. The limit of quantification
190 (LOQ) for each gene was determined according to Bustin et al. (2009) and was: 1548, 36, 122,
191 217, and 112 copy μL^{-1} for 16S rRNA, *sul2*, *tetA*, *qnrS*, and *intI1* genes, respectively. Template
192 dilutions were used to ensure that there was no inhibition of the PCR reaction (Di Cesare et al.,
193 2013). Gene abundances were reported relative to the copy numbers of the 16S rRNA gene in the
194 same sample. In order to evaluate if the treatment affected the dynamics of resistance genes,
195 differences in their abundance were assessed by (i) Multivariate ANOVA (MANOVA),
196 analyzing the total tested ARG load (genes together), and then (ii) for each single gene by
197 ANOVA. For all the analyses, the normalized gene abundances were used as response variables.

198

199 2.7 Bacterial community analyses

200 The V3-V4 region of the 16S rRNA gene was sequenced to obtain a bacterial community profile
201 using the universal bacterial primer pair S-D-Bact-0341-b-S-17/S-D-Bact-0785-a-A-21
202 (Herlemann et al., 2011) on an Illumina platform (MiSeq) at IGA Technology Services Srl
203 (Udine, Italy). Raw reads were deposited at NCBI's sequence read archive (SRA) as project
204 PRJNA772528. Cutadapt 1.9.1 was used to remove adaptors and primers sequences before
205 analysis of the sequencing data (Martin, 2011). The Usearch pipeline was used to filter and
206 merge the sequences, following the instructions of the online tutorial (Edgar, 2010). Unique high
207 quality reads were identified and used as sequence variants to cluster the data into ZOTUs (zero
208 radius operational taxonomic units) with the *unoise* algorithm (Edgar, 2016). The *syntax*

209 command with the SILVA database (Quast et al., 2013) was used to identify taxonomically the
210 sequences, which were confirmed if they were $\geq 80\%$ similar to those in the database. In order to
211 obtain a normalized dataset, all data were rarefied to the read number of the sample with the
212 lowest count (namely 38,883). From the dataset, ZOTUs that were identified as chloroplasts or
213 mitochondria and those not identified at least at a Phylum level were removed (reducing the
214 original dataset from 4277 to 3839 ZOTUs). To investigate differences in bacterial communities
215 between treatments, two datasets were used: 1) the total bacterial community and 2) a subset
216 with only genera containing potentially pathogenic bacteria. The “potentially pathogenic
217 bacteria” were defined as the bacterial genera that also included clinically relevant pathogenic
218 species as reported in the pathogens database of the Bode Science Center ([https://www.bode-](https://www.bode-science-center.com/center/relevant-pathogens-from-a-z.html)
219 [science-center.com/center/relevant-pathogens-from-a-z.html](https://www.bode-science-center.com/center/relevant-pathogens-from-a-z.html)) and previously published (Di
220 Cesare et al., 2020b; Galafassi et al., 2021). For both, the whole community and potentially
221 pathogenic bacteria only we calculated the richness, defined as the number of ZOTUs in each
222 sample. Differences in richness between treated samples and controls were tested using a
223 generalized linear model (GLM), considering a Poisson distribution of the data and a Tukey test
224 as post-hoc analysis. Beta diversity was analyzed by calculating a matrix of all pairwise
225 comparisons of the communities through abundance weighted Bray–Curtis dissimilarity index of
226 the total bacterial community, using the *vegan* package (Oksanen et al., 2007). A dendrogram
227 depicting the clustering of all samples was calculated using hierarchical cluster analysis (*hclust*)
228 with average linkage (**Supplementary Figure S1**). To evaluate if the treatments could contribute
229 to the variance of beta diversity, a PERMANOVA (Permutational ANOVA) was performed
230 using the *vegan* package (Anderson, 2001; Oksanen et al., 2007). Furthermore, to better
231 understand the efficacy of the treatments on the potentially pathogenic genera, their total

232 abundance and the abundance of each genus in treated and controls samples were compared
233 through a GLM (Tukey post-hoc tested). Only the results with p-value <0.05 were plotted,
234 meaning that they were considered significantly different between treatments.

235

236 **3. Results**

237 *3.1 Experiment 1*

238 Cell abundance and vitality in treated WW samples and controls significantly varied during the
239 experiment according to treatments and, most notably, pH values (ANOVA: $p \leq 1.0 \times 10^{-9}$;
240 **Supplementary Table S4 and S5**) (**Figure 2**). In particular, at T0 the mere acidification of WW
241 to pH 5 significantly reduced cell numbers and vitality (**Figure 2, Supplementary Table S4 and**
242 **S6**). Hereinafter, ‘treatments’ are referred to acidification followed by addition of H₂O₂ or ZVI +
243 H₂O₂ (ZVI-Fenton), ‘controls’ to acidification alone. At the end of the experiment, after
244 incubation and neutralization, no differences in terms of cell abundance were observed between
245 treatments in the same acidic condition (*e.g.*, control *vs.* sample treated with H₂O₂, both acidified
246 with H₃PO₄ at pH 5), nor when comparing similar treatments in slightly different conditions
247 (*e.g.*, sample treated with ZVI + H₂O₂, acidified with H₃PO₄ at pH 5, *vs.* sample treated with ZVI
248 + H₂O₂, acidified with H₂SO₄ at pH 5) (**Figure 2a, Supplementary Table S4**). On the contrary,
249 looking at cell vitality at T90S, the treatment with ZVI + H₂O₂ of the sample acidified with
250 H₃PO₄ at pH 5 (*i.e.*, 90 min contact time with ZVI + H₂O₂ in these conditions) significantly
251 increased the percentage of damaged bacteria both in respect with its control, and in respect with
252 the same treatment at different pH (H₃PO₄, pH 6) (**Figure 2b, Supplementary Table S5**).
253 Starting from these results, the ZVI-Fenton treatment with H₃PO₄ at pH 5 was selected for the

254 “experiment 2”. All the pairwise comparisons that were significantly different are reported in
255 **Supplementary Table S4** (cell abundance) and **Supplementary Table S5** (percentage of
256 damaged cells).

257 Note that pH 5 was obtained by adding 1.4 mL of a 0.6 M H₃PO₄ stock solution to wastewater,
258 which produced a phosphate concentration that was higher than discharge limits. However, the
259 ZVI-Fenton treatment would be located after secondary WW sedimentation and before the
260 tertiary step of phosphate elimination (Furia et al., 2021), which would remove species with
261 eutrophication potential from the final stream and even favor the recovery of useful compounds
262 (fertilizers) such as struvite from WW.

263

264 *3.2 Experiment 2*

265 *3.2.1 Flow cytometry*

266 Flow cytometric analysis of samples from “experiment 2” confirmed the findings obtained for
267 “experiment 1”. Indeed, significant differences between samples were observed both in terms of
268 cell abundance and vitality (ANOVA: $p \leq 6.36 \times 10^{-6}$; **Figure 3, Supplementary Table S6** and
269 **S8**). There was a significant drop of cell numbers and vitality after acidification of WW, and no
270 variation in cell abundance of the control and treated samples at T90S (**Figure 3,**
271 **Supplementary Table S6**). Again, at the end of the experiment the treatments with H₂O₂ and
272 ZVI + H₂O₂ caused significant increase in the percentage of damaged cells when compared to
273 the control (**Figure 3b, Supplementary Table S7**). All the pairwise comparisons that were
274 significantly different during the experiment are reported in **Supplementary Table S6** (cell
275 abundance) and **Supplementary Table S7** (percentage of damaged cells).

276 3.2.2 Bacterial community composition

277 When considering the whole bacterial community, richness was significantly higher in the
278 control and H₂O₂-treated samples compared to samples treated with ZVI + H₂O₂ (GLM: p =
279 2.2×10^{-16} ; **Figure 4a, Supplementary Table S8**). In contrast, looking at the potentially
280 pathogenic genera only, richness did not show any significant difference between samples
281 (GLM: p= 0.413; **Figure 4b, Supplementary Table S8**). Regarding beta diversity, the treatment
282 explained 48.4% of its variation in the case of the whole bacterial community (**Supplementary**
283 **Figure S2a, Supplementary Table S9**), while the composition of the potential pathogenic
284 bacteria was less influenced (30.8%) by treatment (**Supplementary Figure S2b,**
285 **Supplementary Table S9**). Focusing on the dynamics of potentially pathogenic bacteria, the
286 total abundance of reads associated to these genera was significantly lower in samples treated
287 with H₂O₂ + ZVI if compared to controls (p= 0.0252) and to the H₂O₂ treatment (p= 0.0186)
288 (**Figure 5, Supplementary Table S10**). When it comes to the single genus, *Acinetobacter*,
289 *Legionella* and *Sphingomonas* were less abundant in the control and H₂O₂ + ZVI treated samples
290 in respect with H₂O₂ treatment; *Bacteroides* had lower abundance in H₂O₂ + ZVI treated
291 samples, whereas *Klebsiella* and *Micobacterium* in the control samples;
292 *Clostridium_sensu_strictu_1* was less abundant in the control and H₂O₂ treated samples in
293 respect with H₂O₂ + ZVI treatment; finally, *Prevotella_1* and *Prevotella_9* had higher abundance
294 in the control samples (**Figure 6**). All the pairwise comparisons of potentially pathogenic genera
295 that showed significant differences are reported in **Supplementary Table S11**.

296

297 3.2.3 ARGs and *intI1* gene quantification

298 ARGs were quantifiable in all the samples, with concentrations ranging from 1.14×10^{-3} to 5.99
299 $\times 10^{-2}$ copies/16S rRNA gene copy. In particular, the abundance of *sul2* ranged between $2.62 \times$
300 10^{-2} and 5.99×10^{-2} copies/16S rRNA gene copy; *tetA* between 1.14×10^{-3} and 2.29×10^{-3}
301 copies/16S rRNA gene copy; *qnrS* between 1.75×10^{-2} and 4.67×10^{-2} copies/16S rRNA gene
302 copy (**Supplementary Figure S2**). Also *intI1* was always quantifiable, with concentrations
303 ranging from 3.99×10^{-3} to 5.68×10^{-3} copies/16S rRNA gene copy. No significant differences
304 in gene abundances between treatments were found when analyzing them either collectively
305 (MANOVA: Pillai's trace = 1.1619, F = 1.3864, p = 0.3275) or as single gene (ANOVA: p \geq
306 0.07464; **Supplementary Table S12**).

307

308 4. Discussion

309 In this study we tested the efficacy of ZVI-Fenton as possible disinfection treatment to lower the
310 load of potential human pathogenic bacteria and ARGs. In detail, we performed a first
311 experiment testing the effect of acidification with different acids, *i.e.* H₂SO₄ and H₃PO₄ at
312 different pH values (5 and 6), and of different treatments on a WW bacterial community,
313 comparing ZVI-Fenton to the treatment with only H₂O₂ and to an untreated control. The best
314 performing treatment in terms of cell vitality decrease was ZVI-Fenton, upon acidification with
315 H₃PO₄ at pH 5. Therefore, this treatment was used in a second experiment to improve the
316 analysis on bacterial community composition, as well as ARGs and class 1 integrons abundance.
317 Possible reason for the higher effectiveness of ZVI-Fenton (H₃PO₄) compared to ZVI-Fenton
318 (H₂SO₄) is the fact that phosphate helps the dissolution of Fe species (Wilhelmy et al., 1985): in

319 particular, the ion HPO_4^{2-} binds Fe(III) to form the $\text{Fe}(\text{HPO}_4)^+$ complex, and dissolved Fe is thus
320 more concentrated in ZVI-Fenton (H_3PO_4) compared to ZVI-Fenton (H_2SO_4) (Furia et al., 2021).
321 On the one side, this would cause higher $\bullet\text{OH}$ production (Keenan and Sedlak, 2008; Pan et al.,
322 2020) that could play a role in bacterial inactivation. On the other hand, dissolved inorganic Fe
323 species are toxic to bacteria, unless they are strongly bound by biocompatible organic ligands
324 (Farinelli et al., 2021).

325 From the second experiment we found that, at the end of the process, cell abundance as measured
326 by flow cytometry was not affected by ZVI-Fenton, nor by the treatment with H_2O_2 alone. This
327 result is in agreement with what observed in “experiment 1” and in a previous study that tested
328 another innovative AOP (UVC/ H_2O_2 /Cu-IDS) using H_2O_2 as comparative treatment, where
329 neither treatment significantly affected the total bacterial abundances (Di Cesare et al., 2020b).
330 Furthermore, similar results were also obtained when testing consolidated disinfection processes
331 based on the use of oxidizing species, such as chlorination (Di Cesare et al., 2016b). Although it
332 is extensively reported that $\bullet\text{OH}$ can damage the cell membrane and the DNA (Zhang et al.,
333 2021), extracellular $\bullet\text{OH}$ would not reach DNA because of the high reaction rates with organic
334 compounds, and it would be consumed by the cell membranes (Wu et al., 2021). The flow
335 cytometer cell counting, which is based on the DNA staining with SYBR Green cannot
336 discriminate between intact and damaged bacterial cells, and thus cannot be considered as the
337 only measurement to evaluate whether a treatment is effective or not against bacteria. For this
338 reason, we performed a flow cytometer cell counting based on double staining with SYBR Green
339 and propidium iodide, which can discriminate between intact and damaged cells, i.e. live/dead
340 stain (Amalfitano et al., 2015). ZVI-Fenton significantly decreased cell vitality compared to
341 untreated samples; again, these results were similar to those previously obtained by testing other

342 AOPs (Di Cesare et al., 2020b) and consolidated disinfection treatments such as peracetic acid
343 (Di Cesare et al., 2016b).

344 Looking at the composition of the bacterial communities in treated and untreated samples, it was
345 evident that ZVI-Fenton strongly affected richness, which was significantly lower than that
346 determined for untreated samples and samples treated with H₂O₂ only. This shift is due to
347 different susceptibility of bacterial groups to the disinfection treatment (Di Cesare et al., 2020a),
348 and has previously been reported after treatment by several disinfection processes, *e.g.* ozonation
349 (Alexander et al., 2016; Becerra-Castro et al., 2016), chlorination (Pang et al., 2016), and UV
350 radiation (Becerra-Castro et al., 2016). Furthermore, the treatment explained approximatively
351 50% of the beta diversity. Samples treated with ZVI-Fenton were located in a distinct cluster in
352 the dendrogram obtained after the hierarchical cluster analysis (**Supplementary Figure S1a**),
353 which highlights once more that this AOP strongly affected the structure of the bacterial
354 community.

355 Focusing on the human potentially pathogenic bacteria only, ZVI-Fenton did not affect their
356 richness and was thus not able to carry out undesirable selection of pathogens. Furthermore, this
357 disinfection process was the best performing treatment in our experiment in terms of reduction of
358 the total pathogenic bacterial abundance. Therefore, the results shown here are a first but
359 promising evidence of the possible applicability of ZVI-Fenton as disinfection process, to
360 decrease the content of the total pathogenic bacteria in wastewaters.

361 Going deeper in the pathogenic bacterial community composition, ZVI-Fenton resulted
362 particularly effective against *Bacteroides*, which are relevant human pathogens. Indeed, once
363 outside the gut some *Bacteroides* species can cause bacteremia and abscess formation in multiple
364 body districts, and they are associated with lethality episodes for more than 19% of cases

365 (Wexler, 2007). ZVI-Fenton also significantly decreased the abundance of *Prevotella* compared
366 to the untreated samples. *Prevotella* have frequently been detected in sputum samples of patients
367 affected by cystic fibroses (CF) treated with antibiotics, and are defined as “emerging bacterial
368 pathogens in the context of CF respiratory infection” (Mahenthiralingam, 2014). Furthermore,
369 ZVI-Fenton did not determine the selection of other pathogenic bacteria, *i.e.*, *Legionella*,
370 *Acinetobacter* and *Sphingomonas*, all associated to the formation of biofilm and/or capable to
371 survive within amoebae (Pereira et al., 2017). Indeed, the latter were significantly more abundant
372 in samples treated with only H₂O₂. However, further pathogenic bacteria (*Clostridium*,
373 *Mycobacterium* and *Klebsiella*) were more abundant in samples treated by ZVI-Fenton compared
374 to untreated samples and/or samples treated only with H₂O₂. This means that additional
375 investigations targeting these specific bacterial genera by using ZVI-Fenton are needed.

376 Neither H₂O₂ nor ZVI-Fenton significantly affected the relative abundance of the tested ARGs
377 and *intI1*. This result is in line with previous findings for other disinfection treatments including
378 chlorination, peracetic acid, UV radiation and ozonation, where ARG abundances resulted
379 unchanged or even increased after treatment (Di Cesare et al., 2016b; Galafassi et al., 2021).
380 However, other studies showed that AOPs were effective in decreasing the load of antibiotic
381 resistant bacteria or ARGs (Ferro et al., 2016; Zhou et al., 2020), suggesting that more efforts in
382 setting the ZVI-Fenton process should be done to decrease ARGs in WWs.

383 A final comment is required about process costs and potential ZVI reuse. As shown in
384 **Supplementary Table S13**, reagent costs for ZVI-Fenton with H₃PO₄ at pH 5 would amount to
385 about 0.15 \$ m⁻³, of which the majority (around 0.12 \$ m⁻³) accounted for by H₃PO₄ itself.
386 Because of this issue, operation with H₃PO₄ at pH < 5 would be problematic even if it could be
387 effective in contaminant degradation. ZVI at pH 5 would account for only about 10% of total

388 reagent costs, which means that ZVI reuse is far less critical than H₃PO₄ saving in process
389 economics. Moreover, 0.02 g L⁻¹ ZVI means that treatment of 1 m³ water would require 20 g
390 ZVI, which is not a huge amount. Still, ZVI might be potentially reused for some times because
391 surface oxidation of a ZVI particle produces a layer of Fe(II) oxide that still retains Fenton
392 reactivity (Minella et al., 2016), although with some loss in performance compared to fresh ZVI
393 (Minella et al., 2019). Recovery of ZVI from wastewater at the end of the treatment would also
394 be made easier by its magnetic properties. However, the low ZVI cost should be compared with
395 the unavoidable costs of reuse, to see if the reuse route is economically viable compared to, e.g.,
396 direct employment of spent ZVI as secondary raw material.

397

398 **5. Conclusions**

399 Overall, the results obtained from “experiment 1” and “experiment 2” showed a possible
400 applicability of ZVI-Fenton as promising treatment to achieve some disinfection of pathogens
401 along with decontamination of pollutants. ZVI-Fenton effectively decreased the total viable
402 bacterial numbers and caused a significant reduction in total human pathogenic bacterial
403 abundance. Unfortunately, it was ineffective in removing ARGs and *int11*. However, it is here
404 necessary to underline that we used a target-based molecular approach (qPCR) that quantifies
405 only some ARGs. In contrast, other approaches such as shotgun metagenomics or High
406 Throughput qPCR could better characterize the bacterial community antibiotic resistome, and
407 provide a clearer overview of the effects of ZVI-Fenton on antibiotic resistance. Furthermore,
408 ZVI-Fenton resulted effective in the removal from WW of selected antibiotics reserved for
409 hospital settings (Furia et al., 2021). Therefore, coupling the results obtained by this

410 microbiological study with those previously obtained on antibiotic degradation, it is reasonable
411 to conclude that ZVI-Fenton is a promising process that deserves to be further investigated and
412 tested in order to be included in the processes applied in WWTPs.

413

414 **Acknowledgements**

415 This work was supported by the “Novel wastewater disinfection treatments to mitigate the spread
416 of antibiotic resistance in agriculture-WARFARE” project (grant n° 2018-0995) funded by
417 Cariplo Foundation, and by Università di Torino and Compagnia di San Paolo with the project
418 “Abatement of pharmaceuticals in hospital wastes - ABATEPHARM” (CSTO168282).

419

420 References

- 421 Alexander, J., Knopp, G., Dötsch, A., Wieland, A., Schwartz, T., 2016. Ozone treatment of conditioned
422 wastewater selects antibiotic resistance genes, opportunistic bacteria, and induce strong
423 population shifts. *Sci. Total Environ.* 559, 103–112.
424 <https://doi.org/10.1016/j.scitotenv.2016.03.154>
- 425 Amalfitano, S., Coci, M., Corno, G., Luna, G.M., 2015. A microbial perspective on biological invasions in
426 aquatic ecosystems. *Hydrobiologia* 746, 13–22. <https://doi.org/10.1007/s10750-014-2002-6>
- 427 Anderson, M.J., 2001. A new method for non-parametric multivariate analysis of variance: NON-
428 PARAMETRIC MANOVA FOR ECOLOGY. *Austral Ecology* 26, 32–46.
429 <https://doi.org/10.1111/j.1442-9993.2001.01070.pp.x>
- 430 Arnone, R.D., Perdek Walling, J., 2006. Waterborne pathogens in urban watersheds. *Journal of Water
431 and Health* 5, 149–162. <https://doi.org/10.2166/wh.2006.001>
- 432 Becerra-Castro, C., Macedo, G., Silva, A.M.T., Manaia, C.M., Nunes, O.C., 2016. Proteobacteria become
433 predominant during regrowth after water disinfection. *Sci. Total Environ.* 573, 313–323.
434 <https://doi.org/10.1016/j.scitotenv.2016.08.054>
- 435 Berendonk, T.U., Manaia, C.M., Merlin, C., Fatta-Kassinos, D., Cytryn, E., Walsh, F., Bürgmann, H., Sørum,
436 H., Norström, M., Pons, M.-N., Kreuzinger, N., Huovinen, P., Stefani, S., Schwartz, T., Kisand, V.,
437 Baquero, F., Martinez, J.L., 2015. Tackling antibiotic resistance: the environmental framework.
438 *Nature Reviews Microbiology* 13, 310–317. <https://doi.org/10.1038/nrmicro3439>
- 439 Bustin, S.A., Benes, V., Garson, J.A., Hellemans, J., Huggett, J., Kubista, M., Mueller, R., Nolan, T., Pfaffl,
440 M.W., Shipley, G.L., Vandesompele, J., Wittwer, C.T., 2009. The MIQE guidelines: minimum
441 information for publication of quantitative real-time PCR experiments. *Clin Chem* 55, 611–622.
442 <https://doi.org/10.1373/clinchem.2008.112797>
- 443 Carratalà, A., Dionisio Calado, A., Mattle, M.J., Meierhofer, R., Luzi, S., Kohn, T., 2016. Solar Disinfection
444 of Viruses in Polyethylene Terephthalate Bottles. *Applied and Environmental Microbiology* 82,
445 279–288. <https://doi.org/10.1128/AEM.02897-15>
- 446 Coha, M., Farinelli, G., Tiraferri, A., Minella, M., Vione, D., 2021. Advanced oxidation processes in the
447 removal of organic substances from produced water: Potential, configurations, and research
448 needs. *Chem. Eng. J.* 414, 128668. <https://doi.org/10.1016/j.cej.2021.128668>
- 449 Comninellis, C., Kapalka, A., Malato, S., Parsons, S.A., Poullos, I., Mantzavinos, D., 2008. Advanced
450 oxidation processes for water treatment: advances and trends for R&D. *Journal of Chemical
451 Technology & Biotechnology* 83, 769–776. <https://doi.org/10.1002/jctb.1873>
- 452 Corno, G., Villiger, J., Pernthaler, J., 2013. Coaggregation in a microbial predator–prey system affects
453 competition and trophic transfer efficiency. *Ecology* 94, 870–881. [https://doi.org/10.1890/12-1652.1](https://doi.org/10.1890/12-
454 1652.1)
- 455 Czekalski, N., Gascón Díez, E., Bürgmann, H., 2014. Wastewater as a point source of antibiotic-resistance
456 genes in the sediment of a freshwater lake. *ISME J* 8, 1381–1390.
457 <https://doi.org/10.1038/ismej.2014.8>
- 458 Di Cesare, A., Corno, G., Manaia, C.M., Rizzo, L., 2020a. Impact of disinfection processes on bacterial
459 community in urban wastewater: Should we rethink microbial assessment methods? *Journal of
460 Environmental Chemical Engineering* 8, 104393. <https://doi.org/10.1016/j.jece.2020.104393>
- 461 Di Cesare, A., De Carluccio, M., Eckert, E.M., Fontaneto, D., Fiorentino, A., Corno, G., Prete, P.,
462 Cucciniello, R., Proto, A., Rizzo, L., 2020b. Combination of flow cytometry and molecular analysis
463 to monitor the effect of UVC/H₂O₂ vs UVC/H₂O₂/Cu-IDS processes on pathogens and antibiotic
464 resistant genes in secondary wastewater effluents. *Water Research* 116194.
465 <https://doi.org/10.1016/j.watres.2020.116194>

466 Di Cesare, A., Eckert, E.M., D'Urso, S., Bertoni, R., Gillan, D.C., Wattiez, R., Corno, G., 2016a. Co-
467 occurrence of integrase 1, antibiotic and heavy metal resistance genes in municipal wastewater
468 treatment plants. *Water Res.* 94, 208–214. <https://doi.org/10.1016/j.watres.2016.02.049>

469 Di Cesare, A., Eckert, E.M., Teruggi, A., Fontaneto, D., Bertoni, R., Callieri, C., Corno, G., 2015.
470 Constitutive presence of antibiotic resistance genes within the bacterial community of a large
471 subalpine lake. *Molecular Ecology* 24, 3888–3900. <https://doi.org/10.1111/mec.13293>

472 Di Cesare, A., Fontaneto, D., Doppelbauer, J., Corno, G., 2016b. Fitness and Recovery of Bacterial
473 Communities and Antibiotic Resistance Genes in Urban Wastewaters Exposed to Classical
474 Disinfection Treatments. *Environ. Sci. Technol.* 50, 10153–10161.
475 <https://doi.org/10.1021/acs.est.6b02268>

476 Di Cesare, A., Luna, G.M., Vignaroli, C., Pasquaroli, S., Tota, S., Paroncini, P., Biavasco, F., 2013.
477 Aquaculture Can Promote the Presence and Spread of Antibiotic-Resistant Enterococci in Marine
478 Sediments. *PLOS ONE* 8, e62838. <https://doi.org/10.1371/journal.pone.0062838>

479 Edgar, R.C., 2010. Search and clustering orders of magnitude faster than BLAST. *Bioinformatics* 26, 2460-
480 2461. <https://doi.org/10.1093/bioinformatics/btq461>

481 Edgar, R.C., 2016. UNOISE2: improved error-correction for Illumina 16S and ITS amplicon sequencing.
482 *BioRxiv*. <https://doi.org/10.1101/081257>

483 Farinelli, G., Minella, M., Pazzi, M., Giannakis, S., Pulgarin, C., Vione, D., Tiraferri, A., 2020. Natural iron
484 ligands promote a metal-based oxidation mechanism for the Fenton reaction in water
485 environments. *J. Hazard. Mater.* 393, 122413.
486 <https://doi.org/https://doi.org/10.1016/j.jhazmat.2020.122413>

487 Farinelli, G., Coxa, M., Minella, M., Fabbri, D., Pazzi, M., Vione, D., Tiraferri, A., 2021. Evaluation of
488 Fenton and modified Fenton oxidation coupled with membrane distillation for produced water
489 treatment: Benefits, challenges, and effluent toxicity. *Science of The Total Environment* 796,
490 148953. <https://doi.org/10.1016/j.scitotenv.2021.148953>

491 Ferro, G., Guarino, F., Castiglione, S., Rizzo, L., 2016. Antibiotic resistance spread potential in urban
492 wastewater effluents disinfected by UV/H₂O₂ process. *Science of The Total Environment* 560–
493 561, 29–35. <https://doi.org/10.1016/j.scitotenv.2016.04.047>

494 Fu, F., Dionysiou, D. D., Liu, H., 2014. The use of zero-valent iron for groundwater remediation and
495 wastewater treatment: A review. *J. Hazard. Mater.* 267, 194–205.
496 <https://doi.org/10.1016/j.jhazmat.2013.12.062>

497 Furia, F., Minella, M., Gosetti, F., Turci, F., Sabatino, R., Di Cesare, A., Corno, G., Vione, D., 2021.
498 Elimination from wastewater of antibiotics reserved for hospital settings, with a Fenton process
499 based on zero-valent iron. *Chemosphere* 283, 131170.
500 <https://doi.org/10.1016/j.chemosphere.2021.131170>

501 Galafassi, S., Sabatino, R., Sathicq, M.B., Eckert, E.M., Fontaneto, D., Dalla Fontana, G., Mossotti, R.,
502 Corno, G., Volta, P., Di Cesare, A., 2021. Contribution of microplastic particles to the spread of
503 resistances and pathogenic bacteria in treated wastewaters. *Water Research* 201, 117368.
504 <https://doi.org/10.1016/j.watres.2021.117368>

505 García-Gil, Á., García-Muñoz, R.A., McGuigan, K.G., Marugán, J., 2021. Solar Water Disinfection to
506 Produce Safe Drinking Water: A Review of Parameters, Enhancements, and Modelling
507 Approaches to Make SODIS Faster and Safer. *Molecules* 26, 3431.
508 <https://doi.org/10.3390/molecules26113431>

509 Giannakis, S., Le, T.-T.M., Entenza, J.M., Pulgarin, C., 2018. Solar photo-Fenton disinfection of 11
510 antibiotic-resistant bacteria (ARB) and elimination of representative AR genes. Evidence that
511 antibiotic resistance does not imply resistance to oxidative treatment. *Water Research* 143,
512 334–345. <https://doi.org/10.1016/j.watres.2018.06.062>

513 Giannakis, S., Voumard, M., Grandjean, D., Magnet, A., De Alencastro, L.F., Pulgarin, C., 2016.
514 Micropollutant degradation, bacterial inactivation and regrowth risk in wastewater effluents:
515 Influence of the secondary (pre)treatment on the efficiency of Advanced Oxidation Processes.
516 *Water Res.* 102, 505–515. <https://doi.org/10.1016/j.watres.2016.06.066>

517 Gillings, M.R., Gaze, W.H., Pruden, A., Smalla, K., Tiedje, J.M., Zhu, Y.-G., 2015. Using the class 1
518 integron-integrase gene as a proxy for anthropogenic pollution. *The ISME Journal* 9, 1269–1279.
519 <https://doi.org/10.1038/ismej.2014.226>

520 GilPavas, E., Correa-Sánchez, S., Acosta, D.A., 2019. Using scrap zero valent iron to replace dissolved iron
521 in the Fenton process for textile wastewater treatment: Optimization and assessment of toxicity
522 and biodegradability. *Environmental Pollution* 252, 1709–1718.
523 <https://doi.org/10.1016/j.envpol.2019.06.104>

524 Herlemann, D.P., Labrenz, M., Jürgens, K., Bertilsson, S., Waniek, J.J., Andersson, A.F., 2011. Transitions
525 in bacterial communities along the 2000 km salinity gradient of the Baltic Sea. *ISME J* 5, 1571–
526 1579. <https://doi.org/10.1038/ismej.2011.41>

527 Huang, W., Brigante, M., Wu, F., Mousty, C., Hanna, K., Mailhot, G., 2013. Assessment of the Fe(III)–
528 EDDS Complex in Fenton-Like Processes: From the Radical Formation to the Degradation of
529 Bisphenol A. *Environ. Sci. Technol.* 47, 1952–1959. <https://doi.org/10.1021/es304502y>

530 Huber, M.M., Canonica, S., Park, G.-Y., von Gunten, U., 2003. Oxidation of pharmaceuticals during
531 ozonation and advanced oxidation processes. *Environ Sci Technol* 37, 1016–1024.
532 <https://doi.org/10.1021/es025896h>

533 Joo, S.H., Feitz, A.J., Sedlak, D.L., Waite, T.D., 2005. Quantification of the Oxidizing Capacity of
534 Nanoparticulate Zero-Valent Iron. *Environ. Sci. Technol.* 39, 1263–1268.
535 <https://doi.org/10.1021/es048983d>

536 Keenan, C.R., Sedlak, D.L., 2008. Ligand-Enhanced Reactive Oxidant Generation by Nanoparticulate Zero-
537 Valent Iron and Oxygen. *Environ. Sci. Technol.* 42, 6936–6941.
538 <https://doi.org/10.1021/es801438f>

539 Leonard, A.F.C., Zhang, L., Balfour, A.J., Garside, R., Hawkey, P.M., Murray, A.K., Ukoumunne, O.C., Gaze,
540 W.H., 2018. Exposure to and colonisation by antibiotic-resistant *E. coli* in UK coastal water users:
541 Environmental surveillance, exposure assessment, and epidemiological study (Beach Bum
542 Survey). *Environment International* 114, 326–333. <https://doi.org/10.1016/j.envint.2017.11.003>

543 Li, G., Nie, X., Chen, J., Jiang, Q., An, T., Wong, P.K., Zhang, H., Zhao, H., Yamashita, H., 2015. Enhanced
544 visible-light-driven photocatalytic inactivation of *Escherichia coli* using g-C₃N₄/TiO₂ hybrid
545 photocatalyst synthesized using a hydrothermal-calcination approach. *Water Research* 86, 17–
546 24. <https://doi.org/10.1016/j.watres.2015.05.053>

547 Mahenthalingam, E., 2014. Emerging cystic fibrosis pathogens and the microbiome. *Paediatric
548 Respiratory Reviews*, Royal Society of Medicine – The 27th symposium: Cystic fibrosis in children
549 and adults, 19th November 2013 15, 13–15. <https://doi.org/10.1016/j.prrv.2014.04.006>

550 Martin, M., 2011. Cutadapt removes adapter sequences from high-throughput sequencing reads.
551 *EMBnet journal* 17, 10-12. <https://doi.org/10.14806/ej.17.1.200>

552 McGuigan, K.G., Conroy, R.M., Mosler, H.-J., Preez, M. du, Ubomba-Jaswa, E., Fernandez-Ibañez, P.,
553 2012. Solar water disinfection (SODIS): A review from bench-top to roof-top. *Journal of
554 Hazardous Materials* 235–236, 29–46. <https://doi.org/10.1016/j.jhazmat.2012.07.053>

555 Minella, M., Bertinetti, S., Hanna, K., Minero, C., Vione, D., 2019. Degradation of ibuprofen and phenol
556 with a Fenton-like process triggered by zero-valent iron (ZVI-Fenton). *Environmental Research*
557 179, 108750. <https://doi.org/10.1016/j.envres.2019.108750>

558 Minella, M., De Bellis, N., Gallo, A., Giagnorio, M., Minero, C., Bertinetti, S., Sethi, R., Tiraferri, A., Vione,
559 D., 2018. Coupling of nanofiltration and thermal Fenton reaction for the abatement of

560 carbamazepine in wastewater. *ACS Omega* 3, 9407-9418.
561 <https://doi.org/10.1021/acsomega.8b01055>

562 Minella, M., Sappa, E., Hanna, K., Barsotti, F., Maurino, V., Minero, C., Vione, D., 2016. Considerable
563 Fenton and photo-Fenton reactivity of passivated zero-valent iron. *RSC Adv.* 6, 86752–86761.
564 <https://doi.org/10.1039/C6RA17515E>

565 Mirzaei, A., Chen, Z., Haghghat, F., Yerushalmi, L., 2017. Removal of pharmaceuticals from water by
566 homo/heterogeneous Fenton-type processes - A review. *Chemosphere* 174, 665–688.
567 <https://doi.org/10.1016/j.chemosphere.2017.02.019>

568 Oksanen, J., Kindt, R., Legendre, P., O'Hara, B., Simpson, G.L., Solymos, P., Stevens, M.H.H., Wagner, H.,
569 2007. The vegan package. *Community Ecology Package* 10, 719.

570 Pan, X., Lin, L., Zhang, W., Dong, L., Yang, Y., 2020. Metagenome sequencing to unveil the resistome in a
571 deep subtropical lake on the Yunnan-Guizhou Plateau, China. *Environmental Pollution* 263,
572 114470. <https://doi.org/10.1016/j.envpol.2020.114470>

573 Pang, Y.-C., Xi, J.-Y., Xu, Y., Huo, Z.-Y., Hu, H.-Y., 2016. Shifts of live bacterial community in secondary
574 effluent by chlorine disinfection revealed by Miseq high-throughput sequencing combined with
575 propidium monoazide treatment. *Appl Microbiol Biotechnol* 100, 6435–6446.
576 <https://doi.org/10.1007/s00253-016-7452-5>

577 Pereira, R.P.A., Peplies, J., Höfle, M.G., Brettar, I., 2017. Bacterial community dynamics in a cooling
578 tower with emphasis on pathogenic bacteria and *Legionella* species using universal and genus-
579 specific deep sequencing. *Water Research* 122, 363–376.
580 <https://doi.org/10.1016/j.watres.2017.06.011>

581 Pignatello, J.J., Liu, D., Huston, P., 1999. Evidence for an Additional Oxidant in the Photoassisted Fenton
582 Reaction. *Environ. Sci. Technol.* 33, 1832–1839. <https://doi.org/10.1021/es980969b>

583 Pignatello, J.J., Oliveros, E., MacKay, A., 2006. Advanced Oxidation Processes for Organic Contaminant
584 Destruction Based on the Fenton Reaction and Related Chemistry. *Critical Reviews in*
585 *Environmental Science and Technology* 36, 1–84. <https://doi.org/10.1080/10643380500326564>

586 Quast, C., Pruesse, E., Yilmaz, P., Gerken, J., Schweer, T., Yarza, P., Peplies, J., Glöckner, F.O., 2013. The
587 SILVA ribosomal RNA gene database project: improved data processing and web-based tools.
588 *Nucleic Acids Res* 41, D590–D596. <https://doi.org/10.1093/nar/gks1219>

589 Rezaei, F., Vione, D., 2018. Effect of pH on Zero Valent Iron Performance in Heterogeneous Fenton and
590 Fenton-Like Processes: A Review. *Molecules* 23, 3127.
591 <https://doi.org/10.3390/molecules23123127>

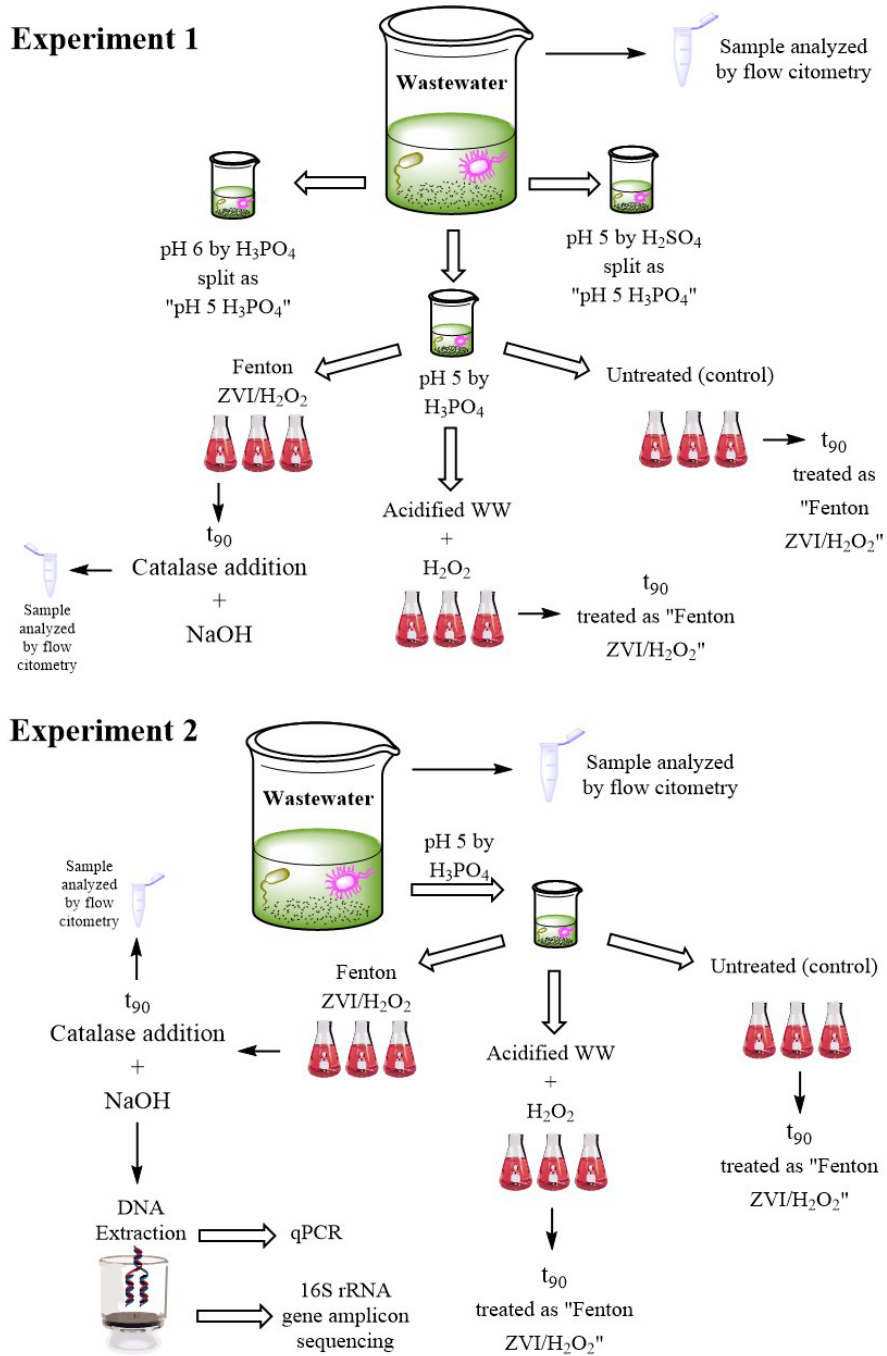
592 Rizzo, L., Manaia, C., Merlin, C., Schwartz, T., Dagot, C., Ploy, M.C., Michael, I., Fatta-Kassinos, D., 2013.
593 Urban wastewater treatment plants as hotspots for antibiotic resistant bacteria and genes
594 spread into the environment: A review. *Science of The Total Environment* 447, 345–360.
595 <https://doi.org/10.1016/j.scitotenv.2013.01.032>

596 Ruales-Lonfat, C., Benítez, N., Sienkiewicz, A., Pulgarín, C., 2014. Deleterious effect of homogeneous and
597 heterogeneous near-neutral photo-Fenton system on *Escherichia coli*. Comparison with photo-
598 catalytic action of TiO₂ during cell envelope disruption. *Applied Catalysis B: Environmental* 160–
599 161, 286–297. <https://doi.org/10.1016/j.apcatb.2014.05.001>

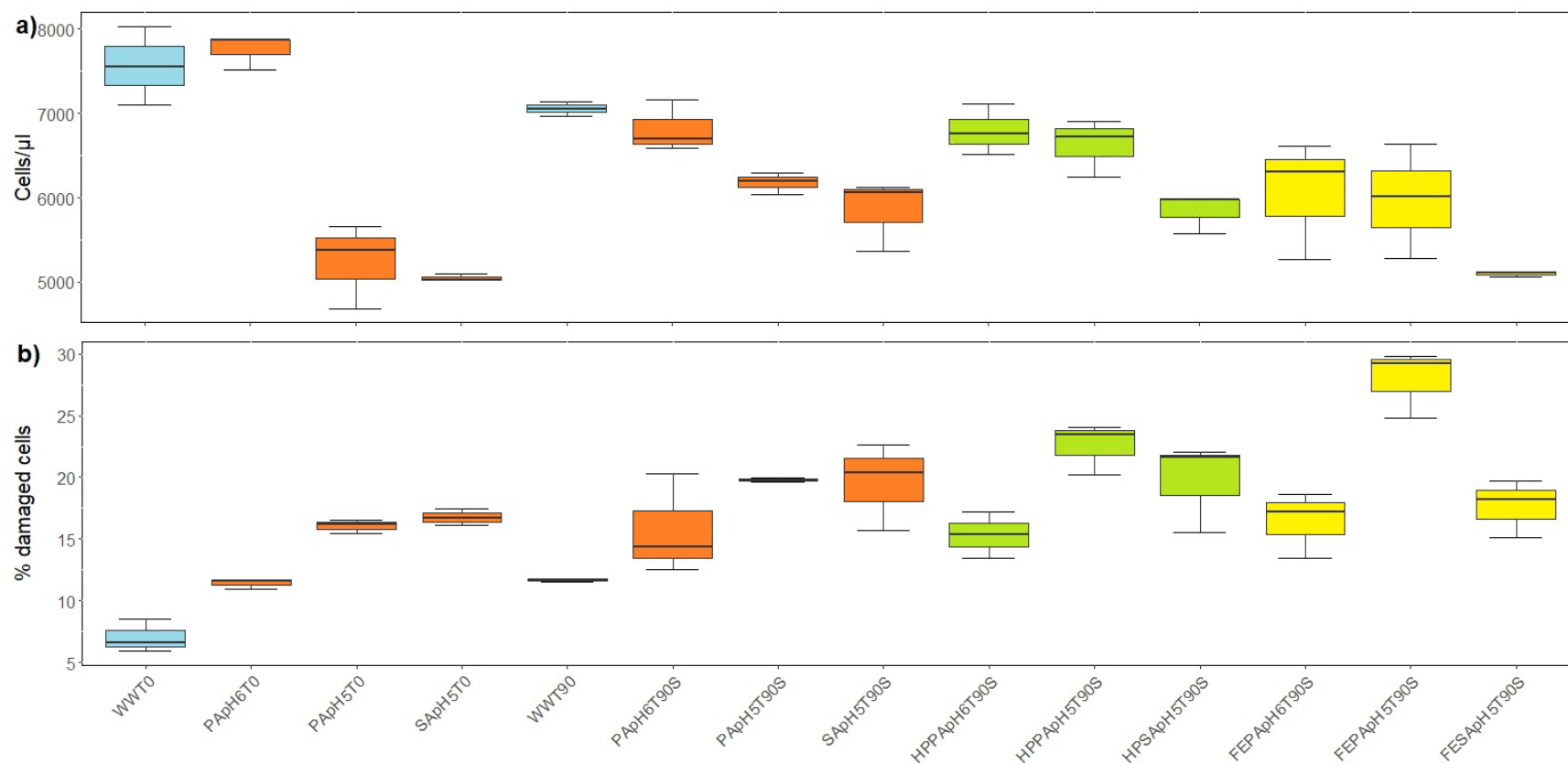
600 Sabatino, R., Di Cesare, A., Dzhenbekova, N., Fontaneto, D., Eckert, E.M., Corno, G., Moncheva, S.,
601 Bertoni, R., Callieri, C., 2020. Spatial distribution of antibiotic and heavy metal resistance genes
602 in the Black Sea. *Marine Pollution Bulletin* 160, 111635.
603 <https://doi.org/10.1016/j.marpolbul.2020.111635>

604 Salgot, M., Huertas, E., Weber, S., Dott, W., Hollender, J., 2006. Wastewater reuse and risk: definition of
605 key objectives. *Desalination, Integrated Concepts in Water Recycling* 187, 29–40.
606 <https://doi.org/10.1016/j.desal.2005.04.065>

607 Shi, Q., Chen, Z., Liu, H., Lu, Y., Li, K., Shi, Y., Mao, Y., Hu, H.-Y., 2021. Efficient synergistic disinfection by
608 ozone, ultraviolet irradiation and chlorine in secondary effluents. *Science of The Total*
609 *Environment* 758, 143641. <https://doi.org/10.1016/j.scitotenv.2020.143641>
610 Tang, J., Wang, J., 2020. Iron-copper bimetallic metal-organic frameworks for efficient Fenton-like
611 degradation of sulfamethoxazole under mild conditions. *Chemosphere* 241, 125002.
612 <https://doi.org/10.1016/j.chemosphere.2019.125002>
613 Vorontsov, A.V., 2019. Advancing Fenton and photo-Fenton water treatment through the catalyst
614 design. *Journal of Hazardous Materials, SI: Photocatalysis:Future Trend* 372, 103–112.
615 <https://doi.org/10.1016/j.jhazmat.2018.04.033>
616 Wang, J., Zhuan, R., 2020. Degradation of antibiotics by advanced oxidation processes: An overview.
617 *Science of The Total Environment* 701, 135023. <https://doi.org/10.1016/j.scitotenv.2019.135023>
618 Wexler, H.M., 2007. Bacteroides: the Good, the Bad, and the Nitty-Gritty. *Clinical Microbiology Reviews*
619 20, 593–621. <https://doi.org/10.1128/CMR.00008-07>
620 Wilhelmy, R.B., Patel, R.C., Matijevic, E., 1985. Thermodynamics and kinetics of aqueous ferric
621 phosphate complex formation. *Inorg. Chem.* 24, 3290–3297.
622 <https://doi.org/10.1021/ic00214a039>
623 Wu, J., Cheng, S., Duan, Y.-Z., Shen, S.-Q., Jiang, B.-C., Li, Y., Shi, P., Li, W.-T., Zhang, Q.-X., Li, A.-M., 2021.
624 Kinetics and efficacy of membrane/DNA damage to *Bacillus subtilis* and autochthonous bacteria
625 during UV/chlorine treatment under different pH and irradiation wavelengths. *Chemical*
626 *Engineering Journal* 422, 129885. <https://doi.org/10.1016/j.cej.2021.129885>
627 Xu, J., Cao, Z., Wang, Y., Zhang, Y., Gao, X., Ahmed, M. B., Zhang, J., Yang, Y., Zhou, J. L., Lowry, G. V.,
628 2019. Distributing sulfidized nanoscale zerovalent iron onto phosphorus functionalized biochar
629 for enhanced removal of antibiotic florfenicol. *Chem. Eng. J.* 359, 713-722.
630 <https://doi.org/10.1016/j.cej.2018.11.180>
631 Zhang, S., Wang, Y., Lu, J., Yu, Z., Song, H., Bond, P.L., Guo, J., 2021. Chlorine disinfection facilitates
632 natural transformation through ROS-mediated oxidative stress. *ISME J* 15, 2969–2985.
633 <https://doi.org/10.1038/s41396-021-00980-4>
634 Zhou, C., Wu, J., Dong, L., Liu, B., Xing, D., Yang, S., Wu, X., Wang, Q., Fan, J., Feng, L., Cao, G., 2020.
635 Removal of antibiotic resistant bacteria and antibiotic resistance genes in wastewater effluent
636 by UV-activated persulfate. *Journal of Hazardous Materials* 388, 122070.
637 <https://doi.org/10.1016/j.jhazmat.2020.122070>
638

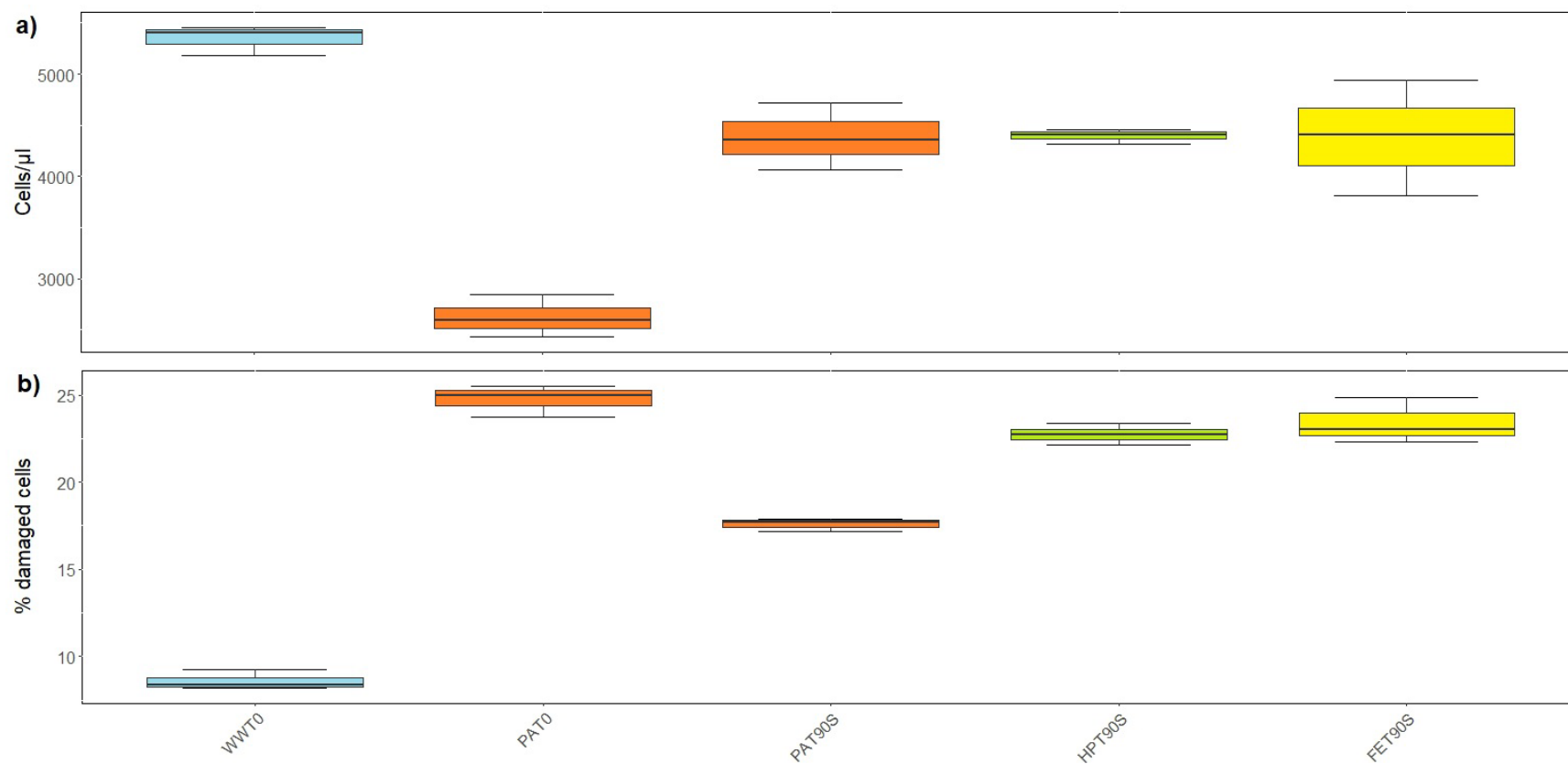


642 **Figure 1.** Illustration of the experimental design used in this work.



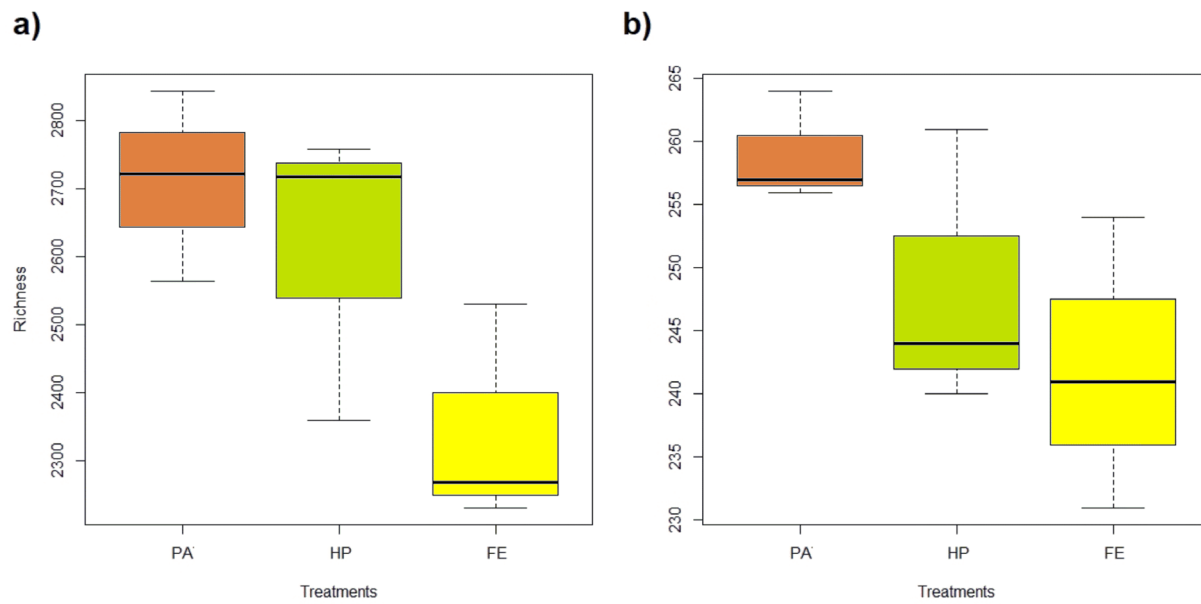
643

644 **Figure 2.** Flow cytometry results of “experiment 1”. **a)** total cell abundance and **b)** percentage of damaged bacteria according to the
 645 different treatments applied throughout the “experiment 1”. Abbreviations: “PA”= phosphoric acid, “SA”= sulfuric acid, “HP”=
 646 hydrogen peroxide, and “FE”= ZVI-Fenton Process. The thick horizontal line represents the median, the box represents 50% of the
 647 values, the whiskers extend to the highest and lowest value within the 1.5 interquartile range.



648
 649 **Figure 3.** Flow cytometry results of “experiment 2”. **a)** Total cell abundance and **b)** percentage of damaged bacteria according to the
 650 different treatments applied throughout the “experiment 2”. Abbreviations: “PA”= phosphoric acid, “HP”= hydrogen peroxide, and
 651 “FE”= ZVI-Fenton Process. The thick horizontal line represents the median, the box represents 50% of the values, the whiskers extend
 652 to the highest and lowest value within the 1.5 interquartile range.

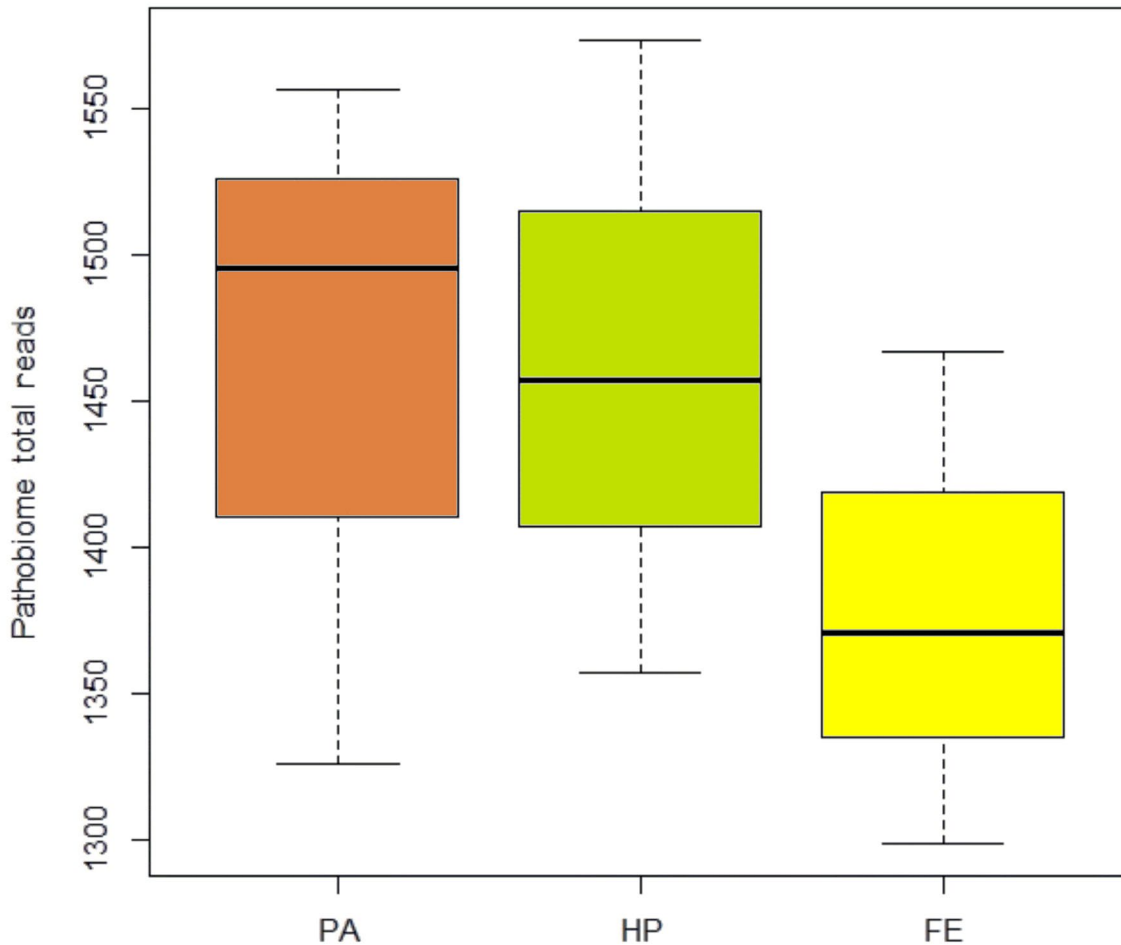
653



654

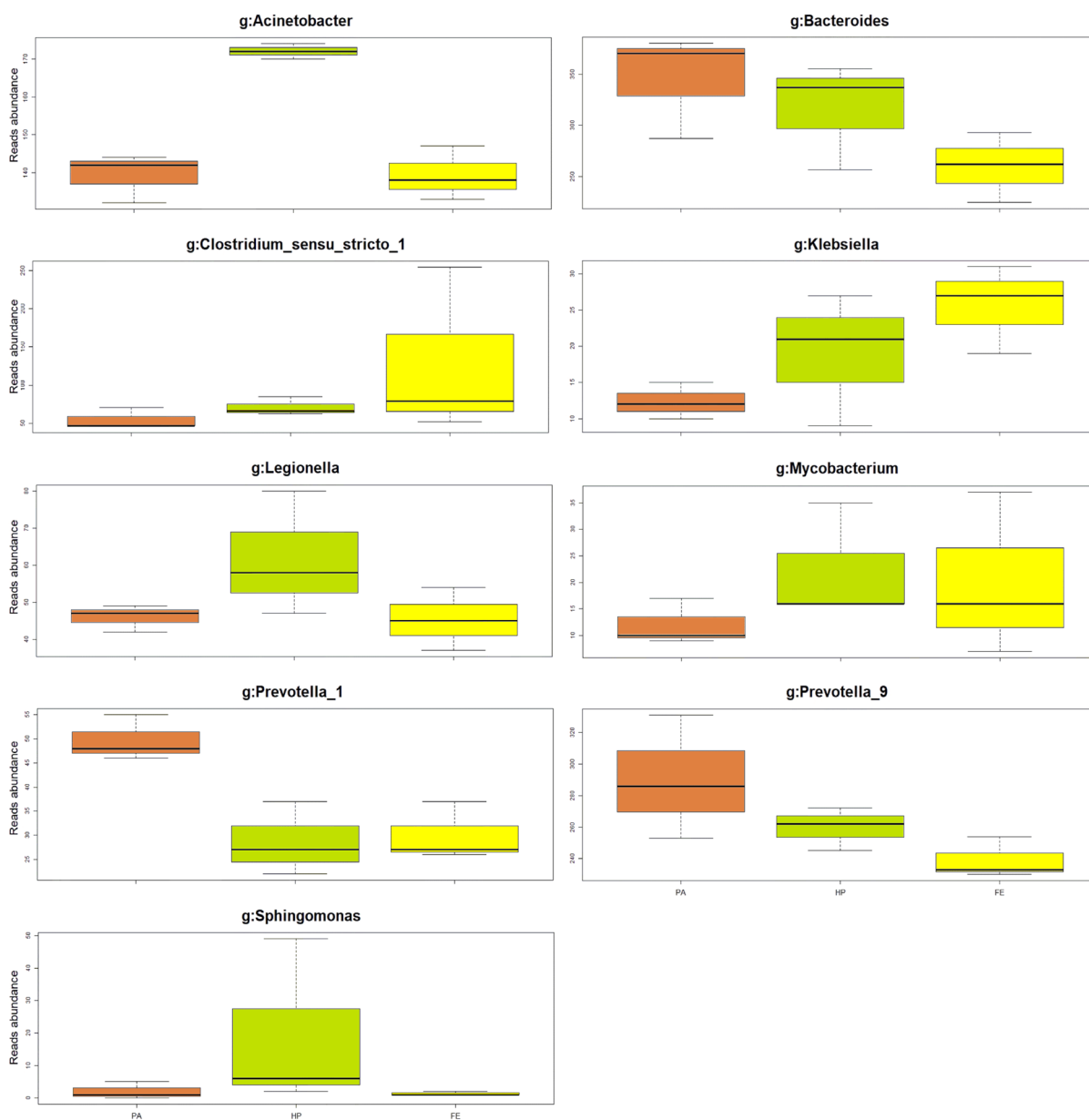
655 **Figure 4.** Richness of “experiment 2” samples. Boxplots of richness of **a)** total bacterial
656 community and **b)** potentially pathogenic genera according to the different treatments.
657 Abbreviations: “PA”= phosphoric acid, “HP”= hydrogen peroxide, and “FE”= ZVI-Fenton
658 Process. The thick horizontal line represents the median, the box represents 50% of the values,
659 the whiskers extend to the highest and lowest value within the 1.5 interquartile range.

660



661

662 **Figure 5.** Total reads abundance associated to the pathobiome. Boxplots of total reads
 663 abundance of potentially pathogenic genera according to the different treatments. Abbreviations:
 664 “PA”= phosphoric acid, “HP”= hydrogen peroxide, and “FE”= ZVI-Fenton Process. The thick
 665 horizontal line represents the median, the box represents 50% of the values, the whiskers extend
 666 to the highest and lowest value within the 1.5 interquartile range.



668

669 **Figure 6.** Reads abundance of potentially pathogenic genera as determined by amplicon
 670 sequencing. Boxplots of reads abundance associated to potentially pathogenic genera according
 671 to the different treatments. Only genera that were significantly different between treatments are
 672 depicted. Abbreviations: “PA”= phosphoric acid, “HP”= hydrogen peroxide, and “FE”= ZVI-
 673 Fenton Process. The thick horizontal line represents the median, the box represents 50% of the
 674 values, the whiskers extend to the highest and lowest value within the 1.5 interquartile range.